

Coupling coefficient observer based on Kalman filter for dynamic wireless charging systems

Nguyen Kien Trung¹, Nguyen Thi Diep²

¹School of Electrical and Electronic Engineering, Hanoi University of Science and Technology, Hanoi, Vietnam

²Faculty of Control and Automation, Electric Power University, Hanoi, Vietnam

Article Info

Article history:

Received Aug 2, 2022

Revised Oct 16, 2022

Accepted Oct 25, 2022

Keywords:

Active rectifier

Dynamic wireless charging

Electric vehicle

Improve efficiency

Kalman filter

ABSTRACT

In the dynamic wireless charging system for electric vehicles, the transfer efficiency reaches the maximum value when the load impedance is equal to the optimal impedance value. However, the optimal impedance value depends on the coupling coefficient, which varies with the electric vehicle's position. Therefore, to track the optimal impedance as well as to improve the transfer efficiency, it is necessary to know the coupling coefficient. This paper proposes a coupling coefficient observer method based on the Kalman filter. Then, on the secondary side, an optimal impedance controller acts on the active rectifier to improve efficiency. The results show that the estimation method achieves high accuracy. The estimated error of the mutual inductance is less than 5% in both the case of impact measurement noise and change system parameters. System efficiency improved by 3.2% compared with the conventional estimation method.

This is an open access article under the [CC BY-SA](https://creativecommons.org/licenses/by-sa/4.0/) license.



Corresponding Author:

Nguyen Thi Diep

Faculty of Control and Automation, Electric Power University

235 Hoang Quoc Viet, Hanoi, Vietnam

Email: diepnt@epu.edu.vn

1. INTRODUCTION

Today, wireless power transfer (WPT) technology is increasingly attractive for industrial applications as well as electric vehicles (EVs) because it simplifies the power supply process and eliminates some of the dangers of electrical leakage for users [1]–[3]. Research is toward applying WPT to charge EVs on the move because it can reduce the battery's capacity and increase the travel distance [4]–[7]. One of the most important criteria in the WPT system is efficiency [8], [9]. Transfer efficiency depends on the compensation circuit, coils, working frequency, and load impedance [1]. When the coil, compensation circuit, and working frequency has designed, the transfer efficiency only depends on the load impedance. The transfer efficiency is maximum only at a load impedance, and it's called the optimal load impedance value [1]. Efficiency drops sharply at other load impedance [10]. And, the load impedance changes according to the state of charge of the battery [11]–[13]. Therefore, impedance matching control is necessary to improve efficiency.

In addition, the optimal load impedance depends on the coupling coefficient. In dynamic wireless charging systems, the coupling coefficient varies with the position of EVs [14]–[16]. Therefore, the problem of estimating the coupling coefficient when the vehicle is moving needs to be done. Many studies have been carried out to estimate the coupling coefficient in the static charging system [17], [18], as well as in the dynamic charging system [19]–[22]. However, these methods only work well under ideal conditions. Under actual operating conditions, the characteristics of the passive elements may be changing, measurements may be affected by noise signal. These conditions make the above estimation methods inaccurate.

The Kalman filter is used to estimate a state variable that is not measurable, or measurable but inaccurate due to the impact of measured noise with high accuracy [23], [24]. Therefore, to overcome the above disadvantages, this paper has proposed a coupling coefficient observer based on the Kalman filter. Firstly, the designed structure of the dynamic charging wireless system is presented. Secondly, the improving transfer efficiency solution is analyzed. Thirdly, a coupling coefficient observer base on the Kalman filter is built. Finally, on the secondary side, an optimal load impedance controller is realized using an active rectifier. The results show that the coupling coefficient is estimated with high accuracy, and the efficiency system is improved.

2. EFFICIENCY-IMPROVING CONTROL BASE

2.1. System structure

Figure 1 shows the proposed dynamic wireless charging system for EVs. The primary side is the modular design, each transmitting module includes a high-frequency inverter that powers the three transmitting coils via LCC compensation circuits. The coils of the transmitting modules are arranged under the roadway to form a dynamic charging lane for EVs. On the secondary side, the receiving coil is mounted under the EVs to receive energy from the dynamic charging lane. An active rectifier is used for optimal impedance control to maximize transfer efficiency. And then, the energy is passed through the battery energy management controller to charge the battery. This paper only considers the problem of wireless power transfer on a transmitting module, not considering issues such as the switching between transmitting modules and battery energy management control.

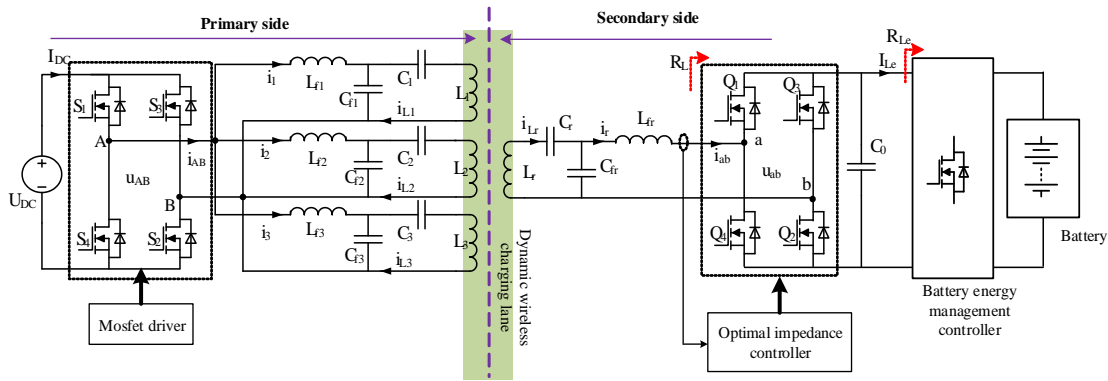


Figure 1. The proposed dynamic wireless charging system

2.2. Solutions to improve transfer efficiency

The LCC compensation circuit has many advantages and is suitable for dynamic charging systems [25]. The double-sided LCC compensation circuit was selected for this system design. Figure 2 shows the equivalent circuit. R_L is the equivalent load impedance from the active rectifier to the battery. The electromagnetic coupling between the coils is represented by the induced voltages. The induced voltage in each coil depends on the value of the mutual inductance and the current in the other coil. Each transmitting coil connects electromagnetically to the other two transmitting coils, and it is replaced by a $j\omega M_{ij}I_{Lj}$ induced voltage. Each transmitting coil connects electromagnetically to the receiving coil and it is replaced by a $j\omega M_{ir}I_{Lr}$ induced voltage. The receiving coil connects electromagnetically to the three transmitting coils and it is replaced by $j\omega M_{ri}I_{Li}$ induced voltage [25]. The transfer efficiency can be calculated as (1) [25].

$$\eta = \frac{R_L I_{Lr}^2}{R_L I_{Lr}^2 + R_r I_{Lr}^2 + R_1 I_{L1}^2 + R_2 I_{L2}^2 + R_3 I_{L3}^2} = \frac{R_L}{R_L^2 \frac{R_r}{\omega^2 L_{fr}^2} + \frac{3 + k_r^2 Q_i Q_r}{k_r^2 Q_i Q_r} + R_L \left(1 + \frac{6}{k_r^2 Q_i Q_r}\right) + \frac{3\omega^2 L_{fr}^2}{R_r} \frac{1}{k_r^2 Q_i Q_r}} \quad (1)$$

Where, $Q_i = \omega L_i / R_i$, $Q_r = \omega L_r / R_r$ are the quality factors of the transmitting and receiving coils, respectively; k_r is the coupling coefficient. The (1) shows that with a designed system working at the resonant frequency, the transfer efficiency depends on the equivalent impedance load. Solving in (2) obtains the maximum transfer efficiency as shown in (3).

$$\frac{\partial \eta}{\partial R_L} = 0 \text{ and } \frac{\partial \eta^2}{\partial R_L^2} < 0 \quad (2)$$

The maximum transfer efficiency is determined by (3).

$$\eta_{max} = \frac{k_r^2 Q_i Q_r}{(\sqrt{3} + \sqrt{3 + k_r^2 Q_i Q_r})^2} \quad (3)$$

Is achieved at (4).

$$R_{L,opt} = \frac{\omega^2 L_{fr}^2}{R_r} \sqrt{\frac{3}{3 + k_r^2 Q_i Q_r}} \quad (4)$$

The (3) and (4) show that when the equivalent load impedance ($R_{L,opt}$) is the optimal load, transfer efficiency is maximum. According to (4), the optimal load depends on the coupling coefficient. However, in a dynamic wireless charging system, the coupling coefficient depends on the EV's position. Therefore, an estimation of the coupling coefficient value is necessary to improve transfer efficiency.

To estimate the coupling coefficient, perform an equivalent circuit analysis of the system at resonance condition in Figure 2. Study [22] has presented a method to estimate the coupling coefficient using the (5).

$$k_r = \frac{L_{fr}}{U_{AB} \sqrt{L_i L_r}} \left[\frac{R_r}{\omega L_{fr}} U_{ab} + \omega L_{fr} I_{Lfr} \right] \quad (5)$$

According to (5), if the r.m.s. of the voltage (U_{ab}) and current (I_{Lfr}) are measured, the coupling coefficient can be estimated. However, (5) is established under ideal conditions, if the parameters of the passive elements change, the accuracy of the estimation method decreases.

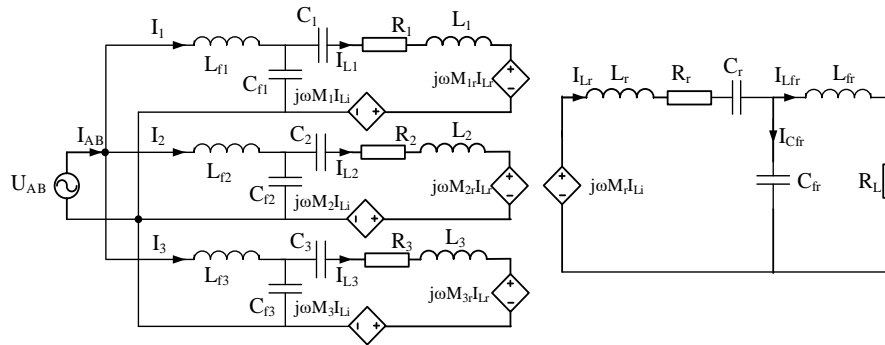


Figure 2. Equivalent circuit

2.3. Building the coupling coefficient observer based on the Kalman filter

The target of controlling the load impedance according to the optimal load is only possible when the coupling coefficient is known. However, the conventional estimation method only works well under ideal conditions. Under actual operating conditions, the characteristics of the passive elements may change, which reduces the accuracy of the estimation method. This section proposes a method to observe the coupling coefficient based on the Kalman filter, which overcomes the above disadvantages.

2.3.1. System modeling

The induced voltage on the receiving coil is performed as follows.

$$E = \omega M_r I_{Li} \quad (6)$$

Where M_r is mutual induction of transmitting coils with receiving coil ($M_r = k_r \sqrt{L_i L_r}$).

The resonant current in the transmitting coils is the same [25].

$$I_{Li} = -j\omega C_{fi} U_{AB} \quad (7)$$

Where U_{AB} is the r.m.s of the output voltage inverter at the primary side. In (7) shows that the resonant current on the transmitting coil is independent of the parameters on the primary side. When the transmitting power was kept fixed, the resonant current is constant. Therefore, the mutual induction (M_r) can estimate by estimating the value of the induced voltage (E) as in the (8).

$$M_r = \frac{E}{\omega L_i} \quad (8)$$

On the secondary side, the Kirchhoff equations are written for the equivalent circuit in Figure 2 as follows:

$$\begin{cases} L_r \frac{di_{Lr}}{dt} + u_{Cr} + u_{Cfr} = E \sin(\omega t) \\ C_r \frac{du_{Cr}}{dt} = i_{Lr} \\ C_{fr} \frac{du_{Cfr}}{dt} = i_{Lr} - i_{Lfr} \\ L_{fr} \frac{di_{Lfr}}{dt} + i_{Lfr} R_L = u_{Cfr} \end{cases} \quad (9)$$

Using the first harmonic approximation (FHA) [26], convert current and voltage values into sine and cosine components:

$$x = X \sin(\omega t + \varphi) = x_c \cos(\omega t) + x_s \sin(\omega t) \quad (10)$$

Derivative of sine and cosine components:

$$\frac{dx}{dt} = \left(\frac{dx_c}{dt} + \omega x_s \right) \cos(\omega t) + \left(\frac{dx_s}{dt} - \omega x_c \right) \sin(\omega t) \quad (11)$$

Rewrite the (9) in terms of cosine and sine components:

$$\begin{cases} L_r \left(\frac{di_{Lr,c}}{dt} + \omega i_{Lr,s} \right) + u_{Cr,c} + u_{Cfr,c} = 0; \\ L_r \left(\frac{di_{Lr,s}}{dt} - \omega i_{Lr,c} \right) + u_{Cr,s} + u_{Cfr,s} = E \\ C_r \left(\frac{du_{Cr,c}}{dt} + \omega u_{Cr,s} \right) = i_{Lr,c}; \\ C_r \left(\frac{du_{Cr,s}}{dt} - \omega u_{Cr,c} \right) = i_{Lr,s} \\ C_{fr} \left(\frac{du_{Cfr,c}}{dt} + \omega u_{Cfr,s} \right) = i_{Lr,c} - i_{Lfr,c}; \\ C_{fr} \left(\frac{du_{Cfr,s}}{dt} - \omega u_{Cfr,c} \right) = i_{Lr,s} - i_{Lfr,s} \\ L_{fr} \left(\frac{di_{Lfr,c}}{dt} + \omega i_{Lfr,s} \right) + i_{Lfr,c} R_L = u_{Cfr,c}; \\ L_{fr} \left(\frac{di_{Lfr,s}}{dt} + \omega i_{Lfr,c} \right) + i_{Lfr,s} R_L = u_{Cfr,s} \end{cases} \quad (12)$$

State variables are set as shown in Table 1. The state model represents the kinematics of the system:

$$\begin{cases} \dot{x}_1 = -\frac{1}{L_r} x_3 - \frac{1}{L_r} x_5 - \omega x_2 \\ \dot{x}_2 = \omega x_1 - \frac{1}{L_r} x_4 - \frac{1}{L_r} x_6 + \frac{1}{L_r} E \\ \dot{x}_3 = \frac{1}{C_r} x_1 - \omega x_4 \\ \dot{x}_4 = \frac{1}{C_r} x_2 + \omega x_3 \\ \dot{x}_5 = \frac{1}{C_{fr}} x_1 - \omega x_6 - \frac{1}{C_{fr}} x_7 \\ \dot{x}_6 = \frac{1}{C_{fr}} x_2 + \omega x_5 - \frac{1}{C_{fr}} x_8 \\ \dot{x}_7 = \frac{1}{L_{fr}} x_5 - \frac{R_L}{L_{fr}} x_7 - \omega x_8 \\ \dot{x}_8 = \frac{1}{L_{fr}} x_6 - \frac{R_L}{L_{fr}} x_8 + \omega x_7 \end{cases} \quad (13)$$

Consider E to be the 9th state variable (x_9) and to be fixed relative to the rest of the system's state variables at the time of consideration.

$$\dot{x}_9 = \frac{dE}{dt} = 0 \quad (14)$$

Combining (13) and (14), the system model is as follows:

$$\dot{x} = Ax \quad (15)$$

Where:

$$A = \begin{bmatrix} 0 & -\omega & -\theta_1 & 0 & -\theta_1 & 0 & 0 & 0 & 0 \\ \omega & 0 & 0 & -\theta_1 & 0 & -\theta_1 & 0 & 0 & \theta_1 \\ \theta_2 & 0 & 0 & -\omega & 0 & 0 & 0 & 0 & 0 \\ 0 & \theta_2 & \omega & 0 & 0 & 0 & 0 & 0 & 0 \\ \theta_3 & 0 & 0 & 0 & 0 & -\omega & -\theta_3 & 0 & 0 \\ 0 & \theta_3 & 0 & 0 & \omega & 0 & 0 & -\theta_3 & 0 \\ 0 & 0 & 0 & 0 & \theta_4 & 0 & -R_L\theta_4 & -\omega & 0 \\ 0 & 0 & 0 & 0 & 0 & \theta_4 & \omega & -R_L\theta_4 & 0 \\ 0 & 0 & 0 & 0 & 0 & 0 & 0 & 0 & 0 \end{bmatrix} \quad \text{with} \quad \begin{cases} \theta_1 = \frac{1}{L_r} \\ \theta_2 = \frac{1}{C_r} \\ \theta_3 = \frac{1}{C_{fr}} \\ \theta_4 = \frac{1}{L_{fr}} \end{cases} \quad (16)$$

The parameter R_L changes during charging, so the kinetic model is nonlinear. Implementing the discretization algorithm for each control cycle, the system model will have the form:

$$x_{k+1} = \Phi x_k; \quad \text{with } \Phi = e^{T_s A} \quad (17)$$

Where T_s is the calculation period of the Kalman filter.

Table 1. State variable name table

Parameter	Value							
Variable	$i_{Lr,c}$	$i_{Lr,s}$	$u_{Cr,c}$	$u_{Cr,s}$	$u_{Cfr,c}$	$u_{Cfr,s}$	$i_{Lfr,c}$	$i_{Lfr,s}$
State	x_1	x_2	x_3	x_4	x_5	x_6	x_7	x_8

2.3.2. Apply the Kalman filter to observe the coupling coefficient

The measurand is the r.m.s. of the rectifier input current it is expressed in state variables as follows.

$$y = I_{Lfr}^2 = h(x) = x_7^2 + x_8^2 \quad (18)$$

The Kalman filter consists of two main calculation stages:

- Stage 1: Prediction. Based on the mathematical model, the Kalman filter calculates the values of the next state variables (x_{k+1}) and the deviation of those calculations from reality (P_{k+1}).

$$x_{k+1}^f = \Phi_k x_k \quad (19)$$

$$P_{k+1}^f = \Phi_k P_k \Phi_k^T + Q \quad (20)$$

- Stage 2: Adjustment. The measured signal had sent to the microcontroller (with measurement noise). At this stage, the Kalman gain is updated, and the state variable vector (x_k) and its deviation (P_k) are correct. The Kalman gain, the state variable vector, and the covariance matrix had corrected according to (21)-(23).

$$K_k = P_k^f H_k^T (H_k P_k^f H_k^T + R)^{-1} \quad (21)$$

$$x_k = x_k^f + K_k (y_k - h(x_k^f)) \quad (22)$$

$$P_k = (I - K_k H_k) P_k^f \quad (23)$$

Where, $H_k = \frac{dh(x)}{dx} = 2x_7 + 2x_8$. H_k is the Jacobian matrix of $h(x)$, and H_k is updated after each calculation cycle. Q and R are covariance matrices of the measurement and process noise.

The Kalman filter algorithm diagram is shown in Figure 3. The current in front of the active rectifier (I_{Lfr}) is measured and fed into (22). Kalman filter is based on the state model and the values of state variables in the past and calculates the vector of state variables at present (x_k). The optimal load impedance is estimated based on the coupling coefficient estimation results (4). Then this value is discretized to calculate the matrix A (16). The state variable is calculated according to (19). the Kalman gain is updated, and the state variable vector (x_k) and its deviation (P_k) are correct.

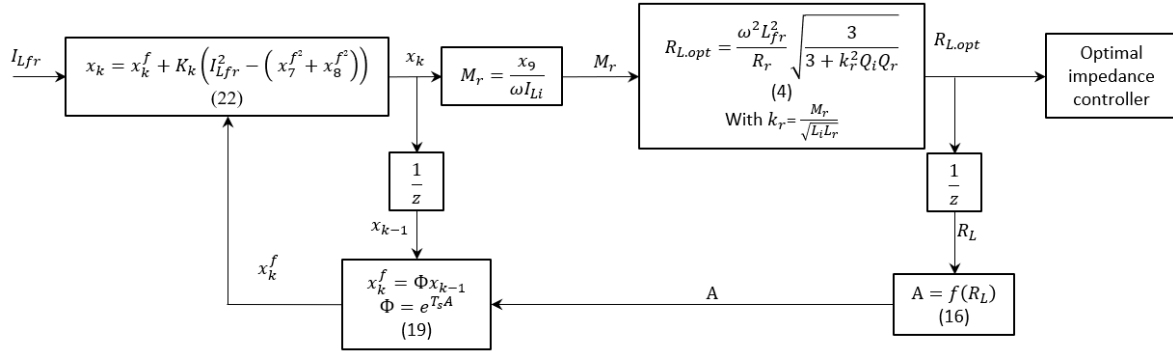


Figure 3. Kalman filter algorithm

2.4. Analysis of impedance conversion method using an active rectifier

Usually, on the secondary side, a diode bridge rectifier and DC/DC converter are used to impedance conversion. This paper proposes to replace it with an active rectifier. This solution reduces one inductance and one filter capacitor. As a result, the size, weight, loss, and cost of the receiver are reduced. Moreover, this paper uses the phase synchronization method combined with a symmetrical phase shift to convert load impedance. The input voltage and current of the active rectifier are phase-synchronized so that the equivalent impedance is purely resistive. Then perform a phase shift to control the load impedance value.

For simplicity of analysis, consider the MOSFET is ideal, ignoring the losses on the filter capacitor C_0 and the capacitor C_0 has a large enough value for the output voltage U_{Le} to be constant. R_{Le} is the equivalent load impedance from the battery energy management controller to the battery. Figure 4(a) is a waveform in an active rectifier. Where, u_{ab}^1 and i_{ab}^1 are the fundamental harmonic component of the input voltage and current of the active rectifier, respectively. V_{Q1} to V_{Q4} are signal turns on MOSFET from Q_1 to Q_4 . The MOSFET turn-on signal has synchronized with the moment when the input current (i_{ab}^1) is zero. In each cycle, there are four switching states and six phases, as shown in Figure 4(b).

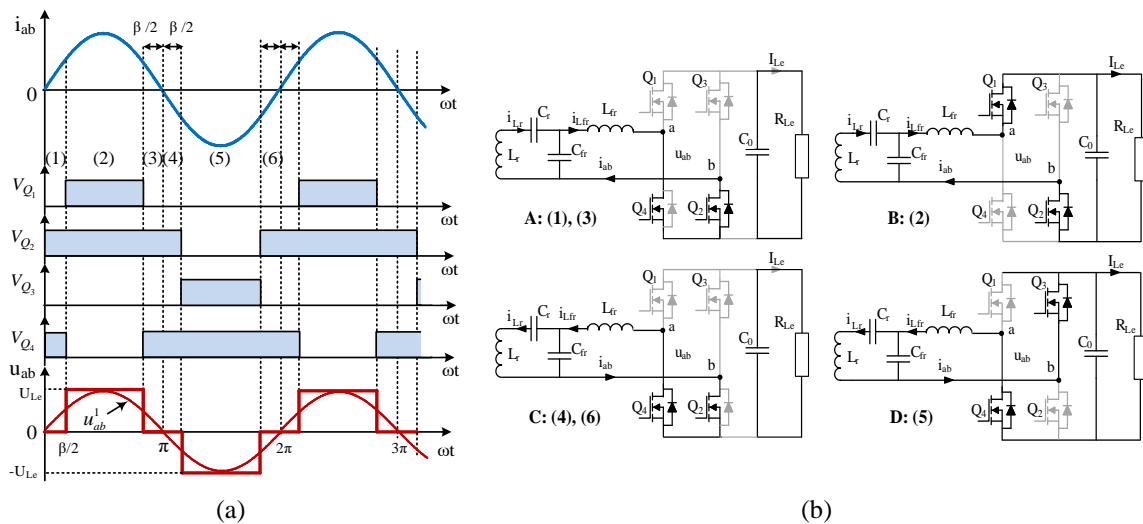


Figure 4. Active rectifier (a) control signal and (b) on/off state of MOSFETs

State A, corresponding to stages (1) and (3): turn on Q_2 and Q_4 . Current i_{ab} flows through Q_2 and Q_4 , and energy is not transferred to the load. Therefore, voltage u_{ab} and current I_{Le} are zero. Energy has accumulated in the capacitor C_0 fed to the load. State B, corresponding to stages (1) and (3): turn on Q_1 and Q_2 . Current i_{ab} flows through Q_1 and Q_2 , and energy is transferred to the load. The analysis is similar for states C and D. Thus, in a cycle, u_{ab} has the values in the (24).

$$u_{ab} = \begin{cases} 0: 0 < \omega t < \beta/2 \\ U_{Le}: \beta/2 < \omega t < \pi - \beta/2 \\ 0: \pi - \beta/2 < \omega t < \pi + \beta/2 \\ -U_{Le}: \pi + \beta/2 < \omega t < 2\pi - \beta/2 \end{cases} \quad (24)$$

Where β is the phase-shift angle; U_{Le} is the output DC voltage of the active rectifier. Based on the fundamental harmonic analysis method, the r.m.s. of u_{ab} is calculated as 25.

$$U_{ab} = \frac{2\sqrt{2}}{\pi} U_{Le} \cos \frac{\beta}{2} \quad (25)$$

Based on the power balance condition, R_L can be calculated as in (26).

$$R_L = \frac{8}{\pi^2} R_{Le} \cos^2 \frac{\beta}{2} \quad (26)$$

In (26) shows that the equivalent load impedance (R_L) can be adjusted by changing the phase shift angle.

Figure 5 shows the block diagram of the optimal impedance controller structure. The r.m.s. of the active rectifier input voltage and current are measured to calculate the equivalent load (R_L) and estimate the optimal load impedance ($R_{L,opt}$) according to the Kalman filter algorithm. The error value is fed to the PI controller. The PI unit calculates the phase shift angle for the active rectifier. In addition, the PLL is used to determine when the current i_{ab} is zero, and to generate a synchronous signal that is fed to a phase shift signal modulator that drives the MOSFETs.

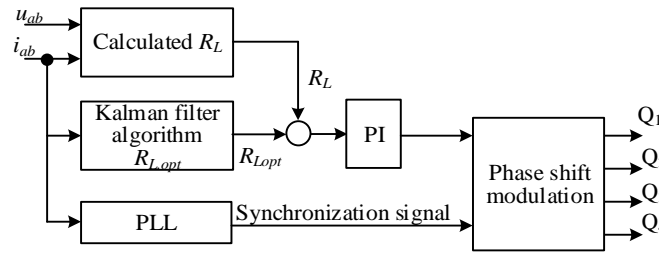


Figure 5. Optimal impedance controller block diagram

3. RESULTS AND DISCUSSION

3.1. Kalman filter verification

A system simulation model is built on MATLAB/Simulink software to verify the accuracy of the Kalman filter. The system parameters are built according to Table 2. The value of the mutual inductance between the transmitting and receiving coils is approximated by the (27).

$$M = M_{tb} + 20\% \cdot M_{tb} \sin(2\pi f_M t) \quad (27)$$

Where $M_{tb} = 16.4443 \mu H$, with a vehicle speed of 40 km/h and a transmitting coil length of 40 cm, M changes with frequency $f_M = 27$ Hz. The mutual inductance characteristic is shown in Figure 6(a). The simulation model considers the impact of measurement noise as in Figure 6(b). The noise source has a frequency of 85 kHz and an amplitude of 10%. The actual and estimated mutual inductance values for several cases are in Figure 7. In case, the system parameters are equal to the original design parameters. The simulation results in Figure 7(a) show that the estimated inductance value follows the real, with an error of less than 5%. In case, system parameters change from the original design parameters. The parameter's value varies according to Table 3. Figure 7(b) shows the estimated results in the three cases as follows.

In case 1, regardless of the impact of measurement noise, the mutual inductance (M) is estimated according to (5). The results show that the estimated error is 14.5%. In case 2, considering the impact of measurement noise, M is estimated according to (5). The results show that the value of M received remains the same as the amplitude of the measured noise, and the estimated error is over 14%. In case 3, considering the impact of measurement noise, M is estimated according to the Kalman filter algorithm. The results show that the value of M follows the actual with an estimated error of less than 5%. Thus, the results of estimating M by

the Kalman filter algorithm have high accuracy in the case of measurement noise impact and the system's parameters change.

Table 2. System parameters

Parameter	Value	Parameter	Value	Parameter	Value
P_0	1.5 kW	L_r	120 μ H	C_2	123.2 nF
U_{DC}	310 V	R_r	0.13 Ω	C_3	95 nF
f_{sw}	85 kHz	L_{fi}	52.6 μ H	L_{fr}	28.9 μ H
L_i	102 μ H	C_{fi}	66.5 nF	C_{fr}	120.9 nF
R_i	0.13 Ω	C_l	93.7 nF	C_r	38.5 nF

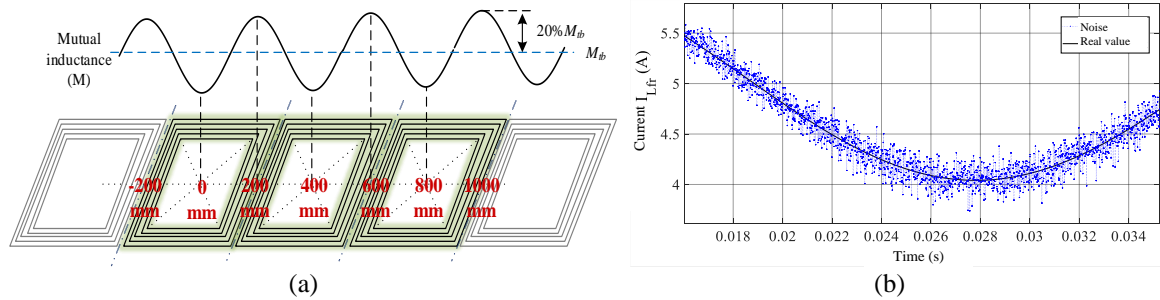


Figure 6. The characteristic (a) mutual inductance approximation and (b) measurement noise

Table 3. System parameters change from the original design parameters

Parameter	L_i	L_{fi}	C_{fi}	C_r	R_i	L_r	R_r
Rate	-5% (down)	-10% (down)	-10% (down)	-6% (down)	15% (up)	-7% (down)	8% (up)

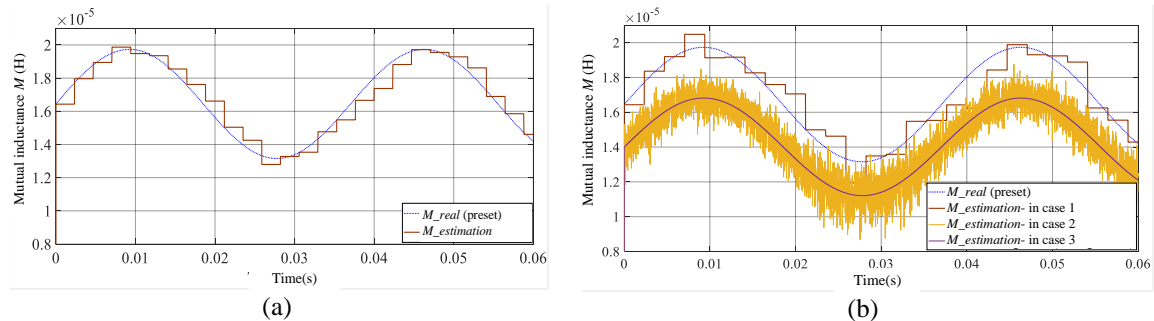


Figure 7. Mutual inductance estimation results (a) original design parameters (b) system parameters change

3.2. Experimental results

An experimental model of dynamic wireless charging with a power of 1.5 kW, transfer distance of 150 mm, and working frequency of 85 kHz was built in the laboratory to verify the proposed method and is shown in Figure 8. The C3M0280090D MOSFET SICs are used to increase the converter efficiency. Polypropylene film capacitors are used as compensating capacitors because of their low loss and high-frequency current tolerance. Ferrite bars are used to increase the electromagnetic connectivity between the transmitting coils and receiving coil.

Figure 9(a) shows the measurement results of the input and output signal of the phase synchronous circuit. The results show that the output pulse of the PLL circuit has accurately captured the phase angle of the current. The pulse is high when the current cuts through zero from negative to positive and is low when the current cuts through zero from positive to negative. Active rectifier input voltage/current are shown in Figure 9(b) which corresponds to the case of phase shift angle of 30 degrees. The results show the active rectifier's ability to control phase shift.

When the equivalent load impedance varies between $80 \Omega \div 130 \Omega$, the load impedance response is shown in Figure 10(a). The optimal impedance ($R_{L,opt}$) is obtained from the results of the Kalman filter algorithm. Although the EV is fixed position, the estimated optimal load impedance changes slightly. It is due to the effect of current and voltage measurement noise. The fluctuation amplitude of the optimal impedance is estimated to be no more than 1%. The results show that the equivalent impedance (R_L) follows the optimal impedance ($R_{L,opt}$) and the static error is less than 1%.

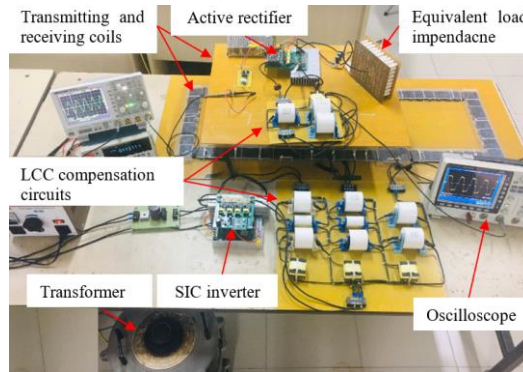


Figure 8. Experimental model

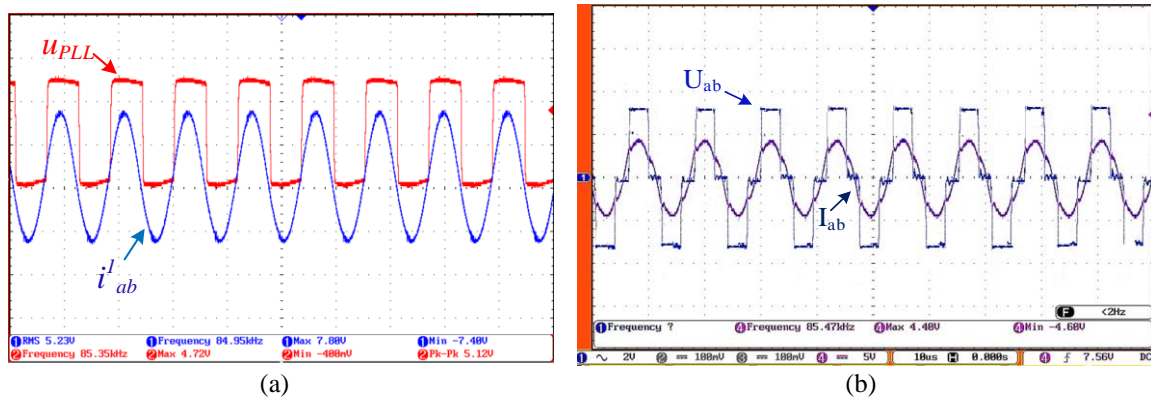


Figure 9. The waveform (a) PLL circuit input and output signals and (b) active rectifier input voltage/current

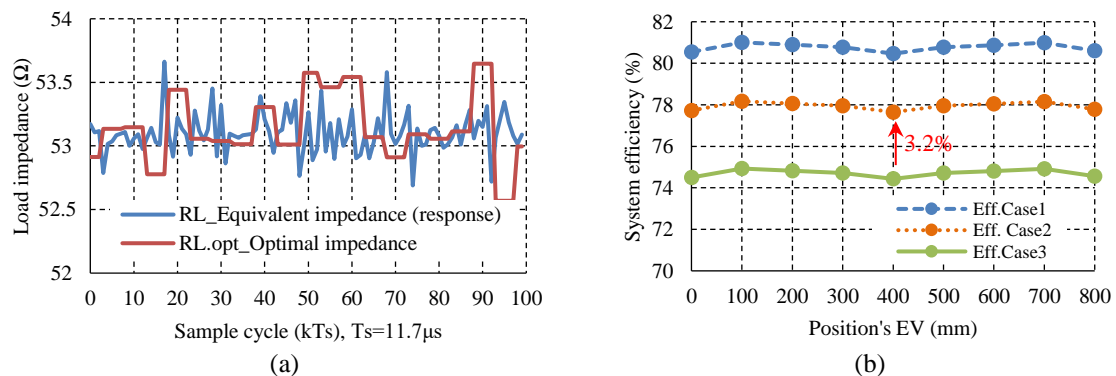


Figure 10. Characteristic (a) load impedance response and (b) system efficiency

When EV moves along a dynamic wireless charging lane, the system efficiency experimental results from the primary inverter input to the equivalent load (R_{Le}) are shown in Figure 10(b). System efficiency includes inverter efficiency, transfer efficiency, and active rectifier efficiency.

- Case 1: system parameters are equal to designed parameters as in Table 2. When the optimal impedance is estimated using the Kalman filter algorithm, the average system efficiency is 80.76%.
- Cases 2 and 3: system parameters are changed as shown in Table 3. When the optimal impedance is estimated using the Kalman algorithm, the average system efficiency is 77.94%. When the optimal impedance is estimated using (5), the average system efficiency is 74.71%. In this case, the system efficiency is improved by 3.2% when using the Kalman filter algorithm.

4. CONCLUSION

The paper proposes to observe the coupling coefficient based on the Kalman filter for dynamic wireless charging systems. The improving transfer efficiency solution is analyzed. The optimal impedance has been estimated through the coupling coefficient estimation, with a static error of less than 1%. Then, the phase synchronous and phase shift methods are used to control the optimal impedance. The results show that the efficiency is improved, and the experimental system efficiency is 80.76%.




REFERENCES

- [1] S. Li and C. C. Mi, "Wireless power transfer for electric vehicle applications," *IEEE J. Emerg. Sel. Topics Power Electron.*, vol. 3, no. 1, pp. 4–17, Mar. 2015, doi: 10.1109/JESTPE.2014.2319453.
- [2] C. Panchal, S. Stegen, and J. Lu, "Review of static and dynamic wireless electric vehicle charging system," *Engineering Science and Technology, an International Journal*, vol. 21, no. 5, pp. 922–937, Oct. 2018, doi: 10.1016/j.jestech.2018.06.015.
- [3] S. Lukic and Z. Pantic, "Cutting the cord: static and dynamic inductive wireless charging of electric vehicles," *IEEE Electrification Mag.*, vol. 1, no. 1, pp. 57–64, Sep. 2013, doi: 10.1109/MELE.2013.2273228.
- [4] G. Buja, C.-T. Rim, and C. C. Mi, "Dynamic charging of electric vehicles by wireless power transfer," *IEEE Trans. Ind. Electron.*, vol. 63, no. 10, pp. 6530–6532, Oct. 2016, doi: 10.1109/TIE.2016.2596238.
- [5] S. Chopra and P. Bauer, "Driving range extension of EV with on-road contactless power transfer—a case study," *IEEE Transactions on Industrial Electronics*, vol. 60, no. 1, pp. 329–338, Jan. 2013, doi: 10.1109/TIE.2011.2182015.
- [6] S. Jeong, Y. J. Jang, and D. Kum, "Economic analysis of the dynamic charging electric vehicle," *IEEE Trans. Power Electron.*, vol. 30, no. 11, pp. 6368–6377, Nov. 2015, doi: 10.1109/TPEL.2015.2424712.
- [7] J. M. Miller, P. T. Jones, J.-M. Li, and O. C. Onar, "ORNL experience and challenges facing dynamic wireless power charging of EV's," *IEEE Circuits Syst. Mag.*, vol. 15, no. 2, pp. 40–53, 2015, doi: 10.1109/MCAS.2015.2419012.
- [8] Q. Zhu, L. Wang, Y. Guo, C. Liao, and F. Li, "Applying LCC compensation network to dynamic wireless EV charging system," *IEEE Trans. Ind. Electron.*, vol. 63, no. 10, pp. 6557–6567, Oct. 2016, doi: 10.1109/TIE.2016.2529561.
- [9] S. Zhou and C. Chris Mi, "Multi-paralleled LCC reactive power compensation networks and their tuning method for electric vehicle dynamic wireless charging," *IEEE Trans. Ind. Electron.*, vol. 63, no. 10, pp. 6546–6556, Oct. 2016, doi: 10.1109/TIE.2015.2512236.
- [10] D. M. Vilathgamuwa and J. P. K. Sampath, "Wireless power transfer (WPT) for electric vehicles (EVs)—present and future trends," in *Plug In Electric Vehicles in Smart Grids*, S. Rajakaruna, F. Shahnia, and A. Ghosh, Eds. Singapore: Springer Singapore, 2015, pp. 33–60. doi: 10.1007/978-981-287-299-9_2.
- [11] M. Chen and G. A. Rincon-Mora, "Accurate electrical battery model capable of predicting runtime and I-V performance," *IEEE Trans. Energy Convers.*, vol. 21, no. 2, pp. 504–511, Jun. 2006, doi: 10.1109/TEC.2006.874229.
- [12] Z. Li, K. Song, J. Jiang, and C. Zhu, "Constant current charging and maximum efficiency tracking control scheme for supercapacitor wireless charging," *IEEE Trans. Power Electron.*, vol. 33, no. 10, pp. 9088–9100, Oct. 2018, doi: 10.1109/TPEL.2018.2793312.
- [13] K. Song, Z. Li, J. Jiang, and C. Zhu, "Constant current/voltage charging operation for series-series and series-parallel compensated wireless power transfer systems employing primary-side controller," *IEEE Trans. Power Electron.*, pp. 1–1, 2017, doi: 10.1109/TPEL.2017.2767099.
- [14] A. Kaminen, M. J. Neath, A. Zaheer, G. A. Covic, and J. T. Boys, "Interoperable EV detection for dynamic wireless charging with existing hardware and free resonance," *IEEE Transactions on Transportation Electrification*, vol. 3, no. 2, pp. 370–379, Jun. 2017, doi: 10.1109/TTE.2016.2631607.
- [15] D. Patil, J. M. Miller, B. Fahimi, P. T. Balsara, and V. Galigekere, "A Coil detection system for dynamic wireless charging of electric vehicle," *IEEE Trans. Transp. Electrification*, vol. 5, no. 4, pp. 988–1003, Dec. 2019, doi: 10.1109/TTE.2019.2905981.
- [16] R. Tavakoli and Z. Pantic, "Analysis, design, and demonstration of a 25-kW dynamic wireless charging system for roadway electric vehicles," *IEEE Journal of Emerging and Selected Topics in Power Electronics*, vol. 6, no. 3, pp. 1378–1393, Sep. 2018, doi: 10.1109/JESTPE.2017.2761763.
- [17] V. Jiwariyavej, T. Imura, and Y. Hori, "Coupling coefficients estimation of wireless power transfer system via magnetic resonance coupling using information from either side of the system," *IEEE J. Emerg. Sel. Topics Power Electron.*, vol. 3, no. 1, pp. 191–200, Mar. 2015, doi: 10.1109/JESTPE.2014.2332056.
- [18] J. Yin, D. Lin, T. Parisini, and S. Y. Hui, "Front-end monitoring of the mutual inductance and load resistance in a series-series compensated wireless power transfer system," *IEEE Trans. Power Electron.*, vol. 31, no. 10, pp. 7339–7352, Oct. 2016, doi: 10.1109/TPEL.2015.2509962.
- [19] D. Kobayashi, T. Imura, and Y. Hori, "Real-time coupling coefficient estimation and maximum efficiency control on dynamic wireless power transfer for electric vehicles," in *2015 IEEE PELS Workshop on Emerging Technologies: Wireless Power (2015 WoW)*, Daejeon, South Korea, Jun. 2015, pp. 1–6. doi: 10.1109/WoW.2015.7132799.
- [20] D. Kobayashi, T. Imura, and Y. Hori, "Real-time coupling coefficient estimation and maximum efficiency control on dynamic wireless power transfer using secondary DC-DC converter," in *IECON 2015 - 41st Annual Conference of the IEEE Industrial Electronics Society*, Yokohama, Nov. 2015, pp. 004650–004655. doi: 10.1109/IECON.2015.7392825.
- [21] N. T. Diep, N. K. Trung, and T. T. Minh, "Maximum efficiency in the dynamic wireless charging systems of electric vehicles," in *2019 10th International Conference on Power Electronics and ECCE Asia (ICPE 2019 - ECCE Asia)*, May 2019, pp. 1–6.




- [22] N. K. Trung and N. T. Diep, "A maximum transfer efficiency tracking method for dynamic wireless charging systems of electric vehicles," *Journal of Electrical and Computer Engineering*, vol. 2021, p. e5562125, Nov. 2021, doi: 10.1155/2021/5562125.
- [23] M. Souaihia, B. Belmadani, and R. Taleb, "A robust state of charge estimation for multiple models of lead acid battery using adaptive extended Kalman filter," *Bulletin of Electrical Engineering and Informatics*, vol. 9, no. 1, Art. no. 1, Feb. 2020, doi: 10.11591/eei.v9i1.1486.
- [24] M. Lagraoui, A. Nejmi, H. Rayhane, and A. Taouni, "Estimation of lithium-ion battery state-of-charge using an extended kalman filter," *Bulletin of Electrical Engineering and Informatics*, vol. 10, no. 4, Art. no. 4, Aug. 2021, doi: 10.11591/eei.v10i4.3082.
- [25] N. T. Diep, N. K. Trung, and T. T. Minh, "Wireless power transfer system design for electric vehicle dynamic charging application," *IJPEDS*, vol. 11, no. 3, p. 1468, Sep. 2020, doi: 10.11591/ijpeds.v11.i3.pp1468-1480.
- [26] H. R. Cha, R. Y. Kim, K. H. Park, and Y. J. Choi, "Modeling and control of double-sided LCC compensation topology with semi-bridgeless active rectifier for inductive power transfer system," *Energies*, vol. 12, no. 20, 2019, doi: 10.3390/en12203921.

BIOGRAPHIES OF AUTHORS



Nguyen Kien Trung    was born in Hanoi, Vietnam. He received the B.E. and M.Sc. degrees in control and automation from Hanoi University of Science and Technology, Vietnam in 2008 and 2011, respectively. In 2016, he received the Ph.D. degree in Functional control systems at Shibaura Institute of Technology, Japan, where he worked as a postdoctoral researcher in 2016-2017. In 2008, he joined the Department of Industrial automation, Hanoi University of Science and Technology. Dr. Trung is a member of the IEEE and IEE of Japan. His current research interests include high frequency converters, Battery charging technology for EV, Battery Management System, and Wireless Power Transfer systems. He can be contacted at email: trung.nguyenkien1@hust.edu.vn.



Nguyen Thi Diep    received Ph.D degree in control and automation from the Hanoi University of Science and Technology, Hanoi, Vietnam in 2021. She is currently working as a Lecturer at Electric Power University, Hanoi, Vietnam. Her current research includes high frequency converters, Battery charging technology for EV, and Wireless Power Transfer systems. She can be contacted at email: diepnt@epu.edu.vn.